Transcriptomic Analysis of Human Podocytes *In Vitro*: Effects of Differentiation and *APOL1* Genotype

Check for updates

Teruhiko Yoshida[1], Khun Zaw Latt[1], Avi Z. Rosenberg[2], Shashi Shrivastav[1], Jurgen Heymann[1], Marc K. Halushka[2], Cheryl A. Winkler[3] and Jeffrey B. Kopp[1]

[1]Kidney Disease Section, Kidney Diseases Branch, National Institute of Diabetes and Digestive and Kidney Diseases, National Institutes of Health, Bethesda, Maryland, USA; [2]Department of Pathology, Johns Hopkins Medical Institutions, Baltimore, Maryland, USA; and [3]Frederick National Laboratory for Cancer Research, National Cancer Institute, National Institutes of Health, Frederick, Maryland, USA

Introduction: The mechanisms in podocytes that mediate the pathologic effects of the *APOL1* high-risk (HR) variants remain incompletely understood, although various molecular and cellular mechanisms have been proposed. We previously established conditionally immortalized human urine-derived podocyte-like epithelial cell (HUPEC) lines to investigate *APOL1* HR variant–induced podocytopathy.

Methods: We conducted comprehensive transcriptomic analysis, including mRNA, microRNA (miRNA), and transfer RNA fragments (tRFs), to characterize the transcriptional profiles in undifferentiated and differentiated HUPEC with *APOL1* HR (G1/G2, 2 cell lines) and *APOL1* low-risk (LR) (G0/G0, 2 cell lines) genotypes. We reanalyzed single-cell RNA-seq data from urinary podocytes from focal segmental glomerulosclerosis (FSGS) subjects to characterize the effect of *APOL1* genotypes on podocyte transcriptomes.

Results: Differential expression analysis showed that the ribosomal pathway was one of the most enriched pathways, suggesting that altered function of the translation initiation machinery may contribute to *APOL1* variant–induced podocyte injury. Expression of genes related to the elongation initiation factor 2 pathway was also enriched in the *APOL1* HR urinary podocytes from single-cell RNA-seq, supporting a prior report on the role of this pathway in *APOL1*-associated cell injury. Expression of microRNA and tRFs were analyzed, and the profile of small RNAs differed by both differentiation status and *APOL1* genotype.

Conclusion: We have profiled the transcriptomic landscape of human podocytes, including mRNA, miRNA, and tRF, to characterize the effects of differentiation and of different *APOL1* genotypes. The candidate pathways, miRNAs, and tRFs described here expand understanding of *APOL1*-associated podocytopathies.

P odocyte injury is a central feature of many primary glomerular diseases and syndromes, including minimal change disease, FSGS, HIV-associated nephropathy, and membranous nephropathy. Podocyte injury may also be present in diverse glomerular diseases associated with systemic disease, including lupus nephritis and diabetes mellitus. Podocytes isolated from humans and mice have a limited replication potential when cultured *in vitro*. We have previously established conditionally immortalized HUPECs and characterized them in 2 states as follows: an undifferentiated state, where podocyte-specific genes were found not to be expressed, and in a differentiated state, where podocyte-specific genes were upregulated and corresponding proteins were observed.[1] HUPECs have been used to investigate various mechanisms in podocytes such as endocytosis[2,3] and cell death.[4]

These cells have been further used to investigate molecular mechanisms of podocyte injury in relationship to *APOL1* HR genotype.[5-9] Although more than 10 years have passed since the discovery of *APOL1* renal risk variants and many mechanisms for effects have

been proposed, it remains unclear which mechanisms in *APOL1* HR genotype cells are most important in driving pathology.[10]

Here, we report on a comprehensive transcriptomic analysis including mRNA, miRNA, and tRFs of 4 undifferentiated and differentiated cell lines in relationship to *APOL1* genotypes.

METHODS

Conditionally Immortalized HUPECs

We have previously generated and characterized HUPECs derived from cells in urine collected from 4 male human subjects as follows[1]: 2 cell lines were from subjects with *APOL1* G0/G0 genotype (one with healthy and the other with HIV-associated FSGS), representing LR genotype, and 2 lines were from subjects with *APOL1* G1/G2 genotype (one with FSGS and the other with HIV-associated nephropathy), representing HR genotype. Urine samples were collected after subjects provided informed consent, under a protocol approved in advance by the National Institute of Diabetes and Digestive and Kidney Disease/National Institutes of Health Intramural Institutional Review Board. Four HUPECs, with distinct *APOL1* genotypes, have been transferred to the American Type Culture Collection (Gaithersburg, MD) and are available to the research community.

Cell Culture and Sample Collection

Human podocytes were immortalized with a temperature-sensitive simian virus 40 T antigen. All cells were studied before passage 15, grown in uncoated tissue culture plasticware. At 33 °C the cells divide, and at 37 °C, the cells enter G0 phase and differentiate.[1] Undifferentiated podocytes were cultured in Roswell Park Memorial Institute 1640 medium (Gibco, ThermoFisher Scientific, Gaithersburg, MD), supplemented with 10% fetal bovine serum and insulin/transferrin/selenium (Gibco, Thermo Fisher Scientific, Gaithersburg, MD) at 33 °C, 95% air and 5% CO_2) for expansion. Podocytes were differentiated by culturing in the same medium formulation at 37 °C for 14 days, exchanging medium every 2 to 3 days. Four podocyte cell lines (3 samples of each, in undifferentiated and differentiated state) were resuspended with QIAzol (QIAGEN, Hilden, Germany) and RNA was extracted (Direct-zol RNA miniprep kit, Zymo Direct, Irvine, CA) (Supplementary Figure S1).

Total RNA Sequencing

Total RNA samples originating from each cell line were sequenced at the Frederick National Laboratory for Cancer Research sequencing facility, National Cancer Institute. Total RNA-seq samples (24) were pooled and sequenced on NovaSeq 6000 SP flow cell following standard workflow (Illumina, San Diego, CA) using Illumina TruSeq Stranded Total RNA Library Prep (Illumina, San Diego, CA) and paired-end sequencing. The samples had 72 to 92 million pass filter reads, with more than 93% of bases above the quality score of Q30. Adapters and low-quality bases were trimmed using Cutadapt v1.18 software[11] before alignment with the human reference genome (hg38 and HIV-1: NC_001802.1) and GENCODE annotation v30 using STAR 2.7.0f.[12] The average mapping rate of all samples was 94%.

Mapping statistics were calculated using Picard 2.18.26 software (Broad Institute, Cambridge, MA). Samples had 0.04% ribosomal bases. The proportion of base categories across all samples were as follows: coding bases, 23% to 39%; untranslated region bases, 22% to 37%; and mRNA bases, 46% to 77%. Library complexity was measured in terms of unique fragments in the mapped reads using Picard's MarkDuplicates utility. The samples had 70% to 80% nonduplicate reads. The sequencing and mapping statistics of total RNA-seq are provided in Supplementary Table S1.

Total RNA Sequencing Analysis

Gene expression quantification analysis was performed for all samples using RNA-seq by expectation optimization (RSEM) v1.3.1 (https://github.com/deweylab/RSEM).[13] Raw count files derived from RSEM were used as input for DESeq2 for differential gene expression analysis. Differential expression tests were conducted using cell line and differentiation status in the analysis. Genes showing differential expression were analyzed by comparisons between differentiation statuses and among *APOL1* genotypes. Gene set enrichment analysis (GSEA v4.1.0) (https://www.gsea-msigdb.org/gsea/license_terms_list.jsp)[14,15] was conducted for 2 comparisons: (i) differentiated *APOL1* LR genotype (G0/G0) podocytes versus undifferentiated *APOL1* LR genotype (G0/G0) podocytes and (ii) differentiated *APOL1* HR genotype (G1/G2) podocytes versus differentiated *APOL1* LR genotype (G0/G0) podocytes. The numbers of enriched gene ontology molecular function pathways (adjusted *P* value <0.05) were identified. VennDiagram and ggplot2 packages in R were used to generate figures by GSEA v4.1.0.

Small RNA Sequencing

Small RNA libraries for Illumina sequencing were prepared as described.[16] In brief, 3′ ligation and 5′ linker-ligation. cDNA generated with Superscript IV reverse transcriptase was amplified with Q5 Polymerase (NEB) in a low cycle PCR (12 cycles), and size-selected libraries were prepared. Pippin Prep (Sage Science, Beverly, MA) was used to remove ligated linker-linker
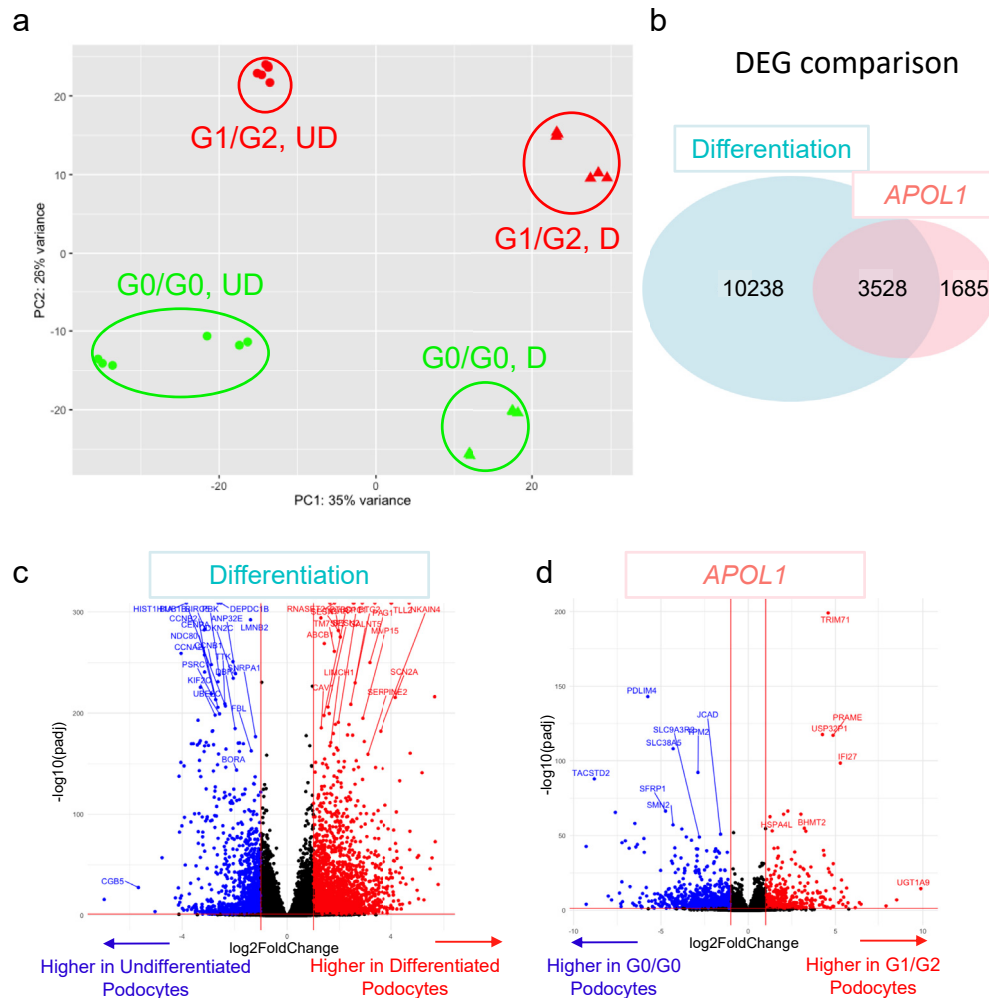
Figure 1. Total RNA-seq of human podocytes compared by differentiation status and *APOL1* genotype. (a) Principal component analysis plot of total RNA-seq results. (b) Venn diagram of differentially expressed genes (FDR q-value < 0.05) comparing differentiation status (D vs. UD) and *APOL1* genotype (HR, G1/G2 vs. LR, G0/G0). (c) Volcano plot of differentially expressed genes by differentiation status. (d) Volcano plot of differential expressed genes by *APOL1* genotype comparison including both differentiation status. (Continued)

(143–185 bp). Pilot PCR using 10% of Pippin-prepped cDNA was performed to determine appropriate number of PCR cycles. TapeStation (Agilent, Santa Clara, CA) was used to determine quality and concentration of the resulting libraries. The samples were sequenced on a HiSeq2500 sequencing system (Illumina, San Diego, CA). The sequencing and mapping statistics of small RNA-seq are provided in Supplementary Table S2.

Small RNA Sequencing Analysis
Mapping statistics are provided in Supplementary Data. Adapter and barcode sequences were removed using Cutadapt v1.16.[11] miRge3.0 was used to count miRNAs and tRFs from small RNA-seq FASTQ files with default parameters.[17] We extracted miR.Counts and tRF.Counts files and used these data for subsequent analysis by DESeq2. Differential expression tests were conducted considering cell line and differentiation status. Differential expression tests were conducted by comparison between differentiation

status and *APOL1* genotype using stringent threshold of miRNA and tRFs >100 reads per million. tRF annotations were conducted as described.[18] VennDiagram and ggplot2 packages in R were used to generate figures.

mRNA-miRNA Combined Analysis
GSEA analysis of total RNA-seq data using the miRNA target prediction database module was conducted to identify candidate miRNAs that might regulate gene expression levels for transcripts identified by total RNA-seq. GSEA analysis was performed using normalized count data from total RNA-seq analysis by DESeq2, with Micro RNA Target Prediction Database microRNA targets as Gene Symbols (c3.mir.-mirdb.v7.4.symbols.gmt). Candidate miRNA lists were made by pairwise comparisons by the threshold of false discovery rate q-value <0.05, as follows: between differentiated *APOL1* LR genotype HUPEC and undifferentiated *APOL1* LR genotype HUPEC, between
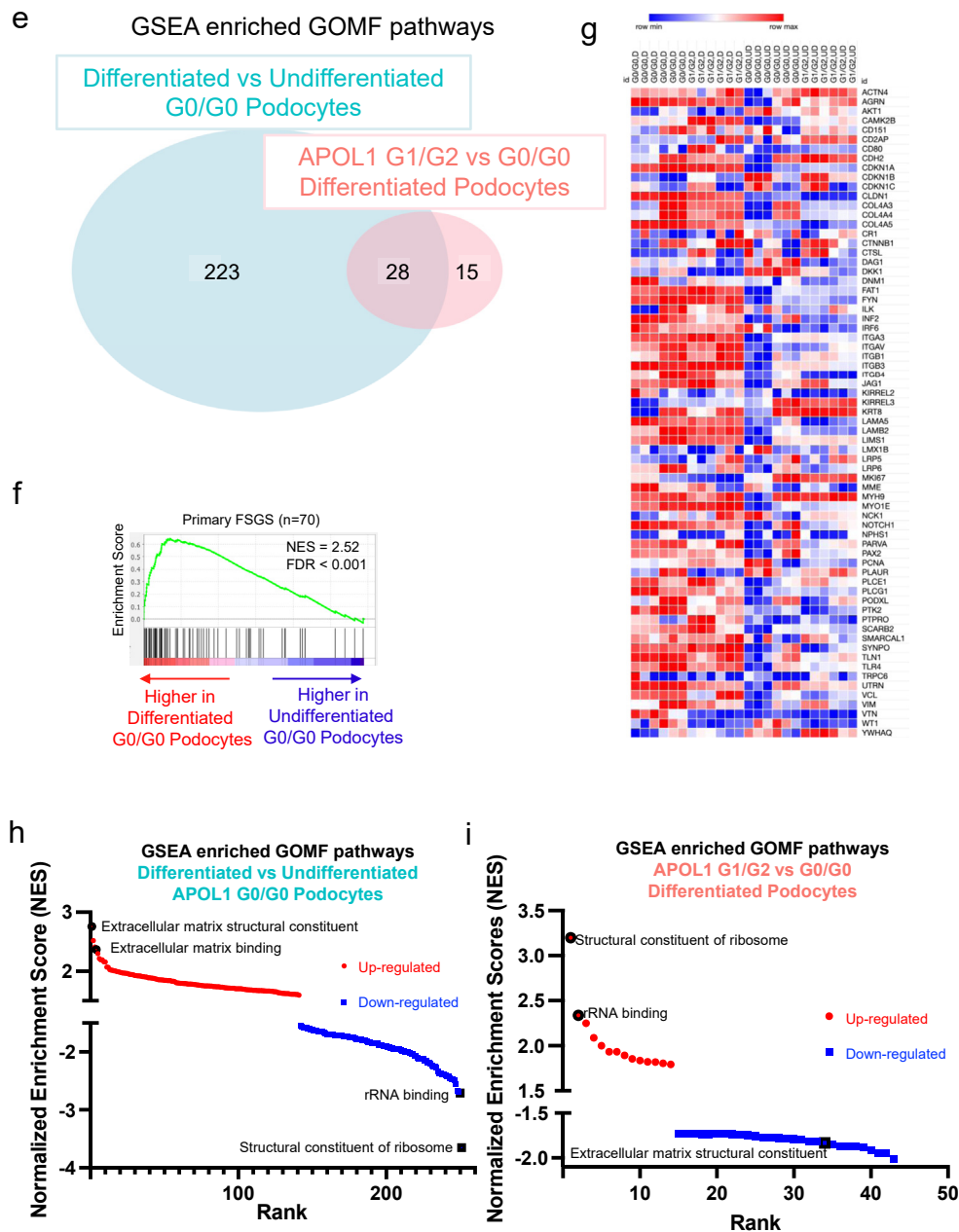
Figure 1. (Continued) (e) Venn diagram of enriched GOMF pathways (FDR q-value < 0.05) by GSEA showing 2 comparisons: differentiated *APOL1* LR genotype (G0/G0) podocytes versus undifferentiated *APOL1* LR genotype (G0/G0) podocytes, differentiated *APOL1* HR genotype (G1/G2) podocytes vs. differentiated *APOL1* LR genotype (G0/G0) podocytes. (f) Enrichment plot of primary FSGS pathway (WP:2572). (g) Heatmap of expressed genes in the primary FSGS pathway (*n* = 70). (h) Enriched GOMF pathways by GSEA comparing differentiated and undifferentiated *APOL1* LR podocytes. (i) Enriched GOMF pathways by GSEA comparing differentiated *APOL1* HR and differentiated *APOL1* LR podocytes. Shown are normalized enrichment scores; red color indicates higher gene expression levels and blue color indicates lower gene expression levels. D, differentiated; FDR, false discovery rate; FSGS, focal segmental glomerulosclerosis; GOMF, gene ontology molecular function; GSEA, gene set enrichment analysis; HR, high-risk; LR, low-risk; UD, undifferentiated.

differentiated *APOL1* HR genotype HUPEC and undifferentiated *APOL1* HR genotype HUPEC, and between differentiated *APOL1* LR genotype HUPEC and differentiated *APOL1* HR genotype HUPEC. Candidate miRNAs on all lists were compared with differentially expressed miRNAs found by small RNA-seq analysis without stringent filtering threshold of miRNA <100 reads per million, so that all miRNAs were included.

Single-Cell RNA Sequencing Data of Urinary Podocytes From FSGS Subjects

We used single-cell gene expression data from the podocyte cluster from published urine single-cell RNA-seq data[19] (GEO accession number GSE176465) to compare podocyte transcriptomes between *APOL1* HR and LR genotype cells. We compared podocyte expression profiles from 7 HR samples (containing a
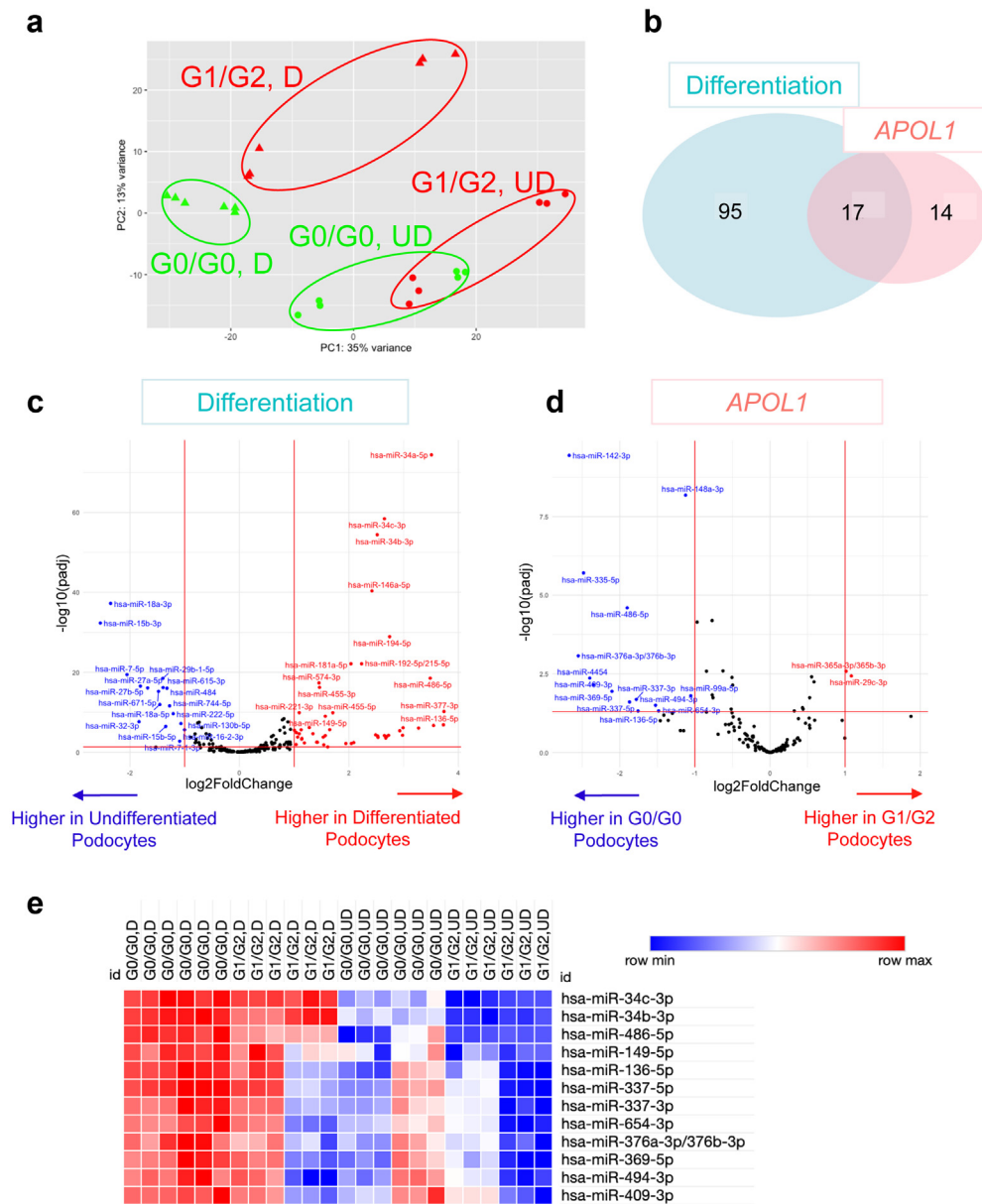
Figure 2. miRNA-seq of human podocytes compared by differentiation and *APOL1* genotype. (a) Principal component analysis plot of miRNA-seq results. (b) Venn diagram of differentially expressed miRNAs (FDR q-value < 0.05), comparing differentiation status (D vs. UD) and *APOL1* genotype (HR vs. LR). (c) Volcano plot of differential expressed miRNAs by differentiation status. (d) Volcano plot of differential expressed miRNAs by *APOL1* genotype. (e) Heatmap of 12 miRNAs that were downregulated by undifferentiated status and *APOL1* HR. D, differentiated; FDR, false discovery rate; HR, high-risk; LR, low-risk; UD, undifferentiated.

total of 226 cells) with those from podocytes from 4 LR samples (103 cells). Differential expression testing was performed in Seurat (v2.3.4). Ingenuity Pathway Analyses (IPA, QIAGEN, Hilden, Germany) were conducted using differentially expressed genes ($P < 0.05$, without correction for multiple testing) as an input.

Network Analysis
Differentially expressed genes, comparing between differentiated APOL1 HR HUPEC and differentiated *APOL1* LR HUPEC by total RNA-seq (adjusted $P < 0.05$), were used as input data (HUPEC gene list). Differentially expressed genes, comparing podocytes from *APOL1* HR

subjects with those from *APOL1* LR subjects by single-cell RNA-seq (adjusted $P < 0.05$) were used as the other input data (urinary podocytes gene list). Gene names and $\log_2$-fold change values were prepared and analyzed by NetworkAnalyst 3.0 (https://networkanalyst.ca/) and ExpressAnalyst (https://www.expressanalyst.ca/).[20] Network building and visualization of 2 gene lists were conducted by NetworkAnalyst 3.0. Intersection of lists were mapped on STRING Interactome (900 Confidence score with experimental evidence) with "Minimum Network" option. Enrichment network analysis was conducted for 2 data sets separately by ExpressAnalyst with over-representation analysis on KEGG database.
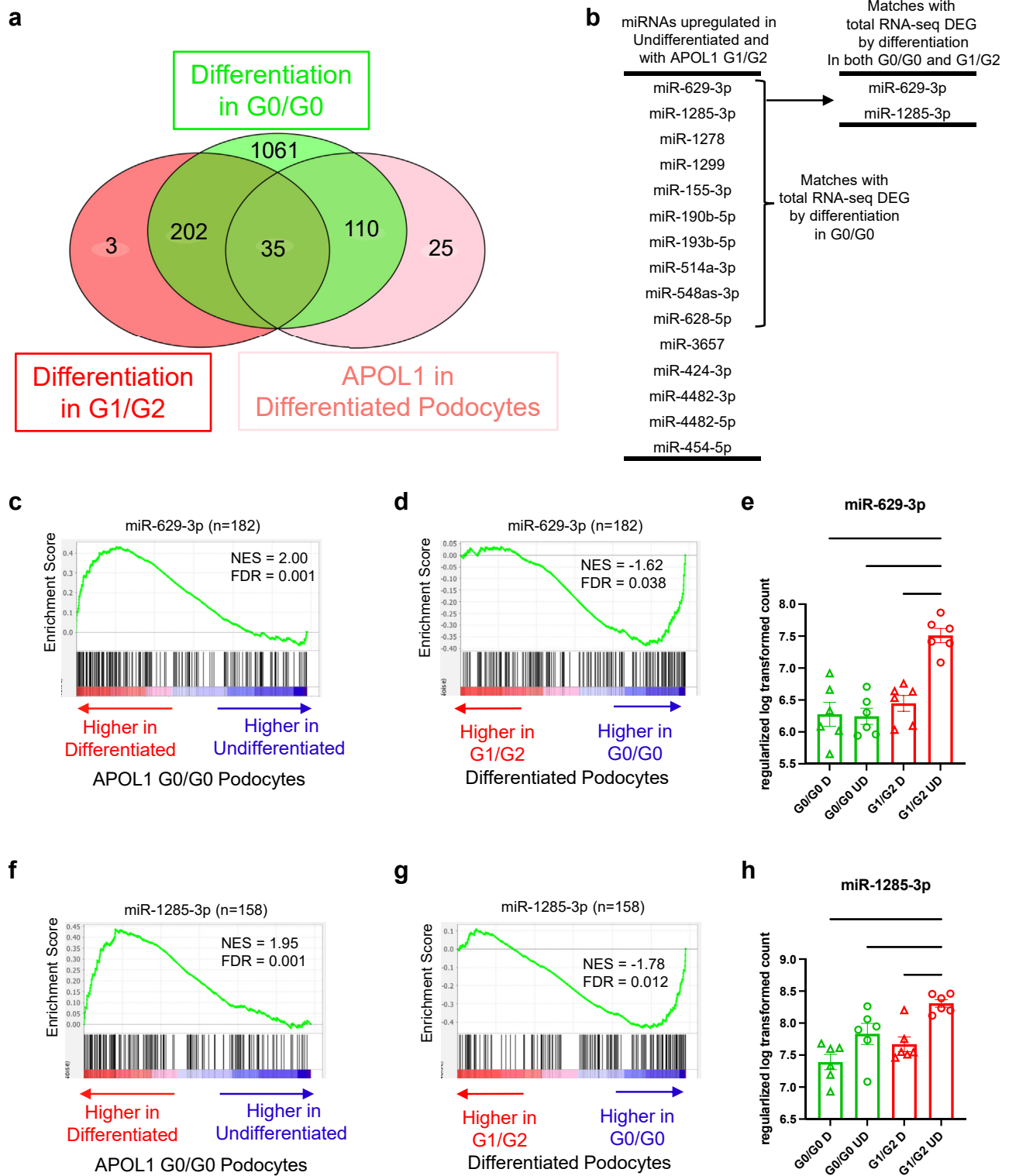
Figure 3. miRNA-mRNA combination analysis. (a) Venn diagram of differentially expressed miRNA candidates by total RNA-seq (FDR q-value < 0.05), comparing differentiation status (D vs. UD) in both APOL1-LR and APOL1-HR podocytes, *APOL1* genotype (HR vs. LR) in differentiated podocytes. (b) List of 15 miRNAs upregulated in undifferentiated and APOL1-HR podocytes by miRNA-seq data, and 2 miRNAs matched with differentially expressed miRNA candidate lists by total RNA-seq by differentiation. (c, d) Enrichment plot of miR-629-3p regulating genes. (e) Relative expression levels of miR-629-3p in each cell line. (f, g) Enrichment plot of miR-1285-3p regulating genes. (h) Shown is relative expression levels of miR-1285-3p in each cell line. D, differentiated; FDR, false discovery rate; HR, high-risk; LR, low-risk; NES, normalized enrichment score; UD, undifferentiated.
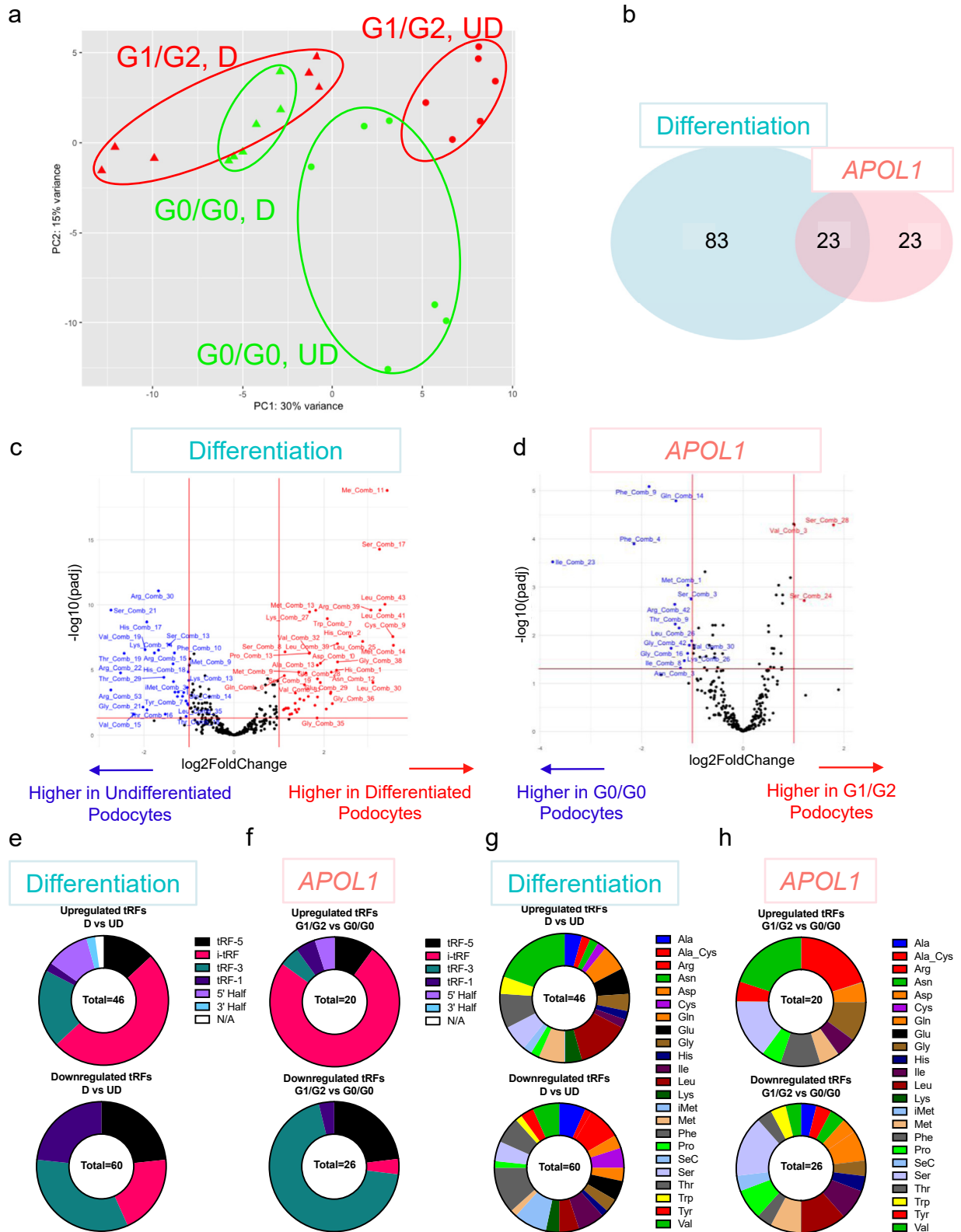
Figure 4. tRF analysis results of human podocytes compared by differentiation and *APOL1* genotype. (a) Principal component analysis plot of tRF results. (b) Venn diagram of differentially expressed tRFs (FDR q-value < 0.05) comparing differentiation status (D vs. UD) and *APOL1* genotype (HR vs. LR). (c) Volcano plot of differential expressed tRFs by differentiation status. (d) Volcano plot of differential expressed tRFs by *APOL1* genotype. (e, f) Differentially expressed tRFs by differentiation status, *APOL1* genotype; categorized by the structural types. (g, h) Differentially expressed tRFs by differentiation status, *APOL1* genotype; categorized by tRNA types. D, differentiated; HR, high-risk; LR, low-risk; tRF, transfer RNA fragment; UD, undifferentiated.

Figure 5. Translational pathways activated by *APOL1* HR in urinary single-cell RNA-seq from FSGS subjects. (a) Shown is a tSNE plot of urinary single-cell RNA-seq data, showing a distinct podocyte cluster. Shown is the urinary single-cell podocyte cluster with podocytes from 23 urine samples of 12 FSGS subjects. (b) Shown is a volcano plot of differentially expressed genes in urinary single-cell RNA-seq podocyte data sets, arranged by *APOL1* genotype. (c) Shown are expression plots of the most highly upregulated genes in *APOL1* HR podocytes, showing stronger expression in the upper portion of the urinary podocyte cluster. (d) Shown are IPA canonical pathway analysis results. These are the top 20 pathways according to −log (*P* value) of urinary single-cell RNA-seq podocyte data sets, presented by *APOL1* genotype comparison. FSGS, focal segmental glomerulosclerosis; HR, high-risk; LR, low-risk; IPA, ingenuity pathway analysis; tSNE, t-distributed stochastic neighbor embedding.

Figure 6. Enrichment network analysis to connect differentially expressed genes comparing *APOL1* HR versus LR from total RNA-seq of human podocytes and from single-cell RNA-seq of urinary podocytes from FSGS subjects. (a) Shown is network visualization of both sets of differentially expressed genes by total RNA-seq comparing differentiated *APOL1* HR human podocytes with differentiated *APOL1* LR human podocytes and by single-cell RNA-seq comparing urinary podocytes from *APOL1* HR subjects with those from *APOL1* LR subjects. The ribosomal and mitochondrial modules are enlarged for better visualization. (b) Shown is enrichment network visualization of differentially expressed genes by total RNA-seq comparing differentiated *APOL1* HR human podocytes with differentiated *APOL1* LR human podocytes. (c) Shown is enrichment network visualization of differentially expressed genes by single-cell RNA-seq comparing urinary podocytes from *APOL1* HR subjects with those from *APOL1* LR subjects. HR, high-risk; LR, low-risk.

Reverse Transcriptase PCR and Quantitative Real-Time PCR

A 0.4-µg aliquot of RNA was used for cDNA synthesis by Superscript II reverse transcriptase for mRNA. Ten nanogram aliquot of RNA was used for cDNA synthesis by miRCURY LNA RT Kit (#339340, QIAGEN, Hilden, Germany) for miRNA. Samples were analyzed by quantitative RT-PCR (qRT-PCR) using FastStart Universal SYBR Green Master (Rox) (#04913850001, Sigma-Aldrich, St. Louis, MO) for mRNA and by miRCURY LNA SYBR Green PCR Kit (#339346, QIAGEN) for miRNA. Relative RNA expression levels in each sample were calculated as ratios relative to the endogenous control RNA (GAPDH for mRNA, U6 for miRNA).

Primer pairs and miRCURY LNA miRNA PCR Assays (#339306, QIAGEN) are listed in Supplementary Table S3.

RESULTS

Total RNA-Seq Demonstrated Substantial Transcriptomic Effects of Podocyte Differentiation and APOL1 Genotype

Principal component analysis plots of total RNA-seq data showed robust clustering and clear separation of global transcriptomic signatures by differentiation status and by *APOL1* genotype (Figure 1a). The numbers of differentially expressed genes (adjusted *P*

value <0.05) from comparisons based on the differentiation status was 13,766 and based on *APOL1* genotypes was 5213 (Figure 1b–d; Supplementary Tables S4 and S5).

To understand specific signatures from each differentiation status and *APOL1* genotype, GSEA analysis was conducted for 2 comparisons: (i) differentiated APOL1 LR genotype (G0/G0) podocytes versus undifferentiated *APOL1* LR genotype (G0/G0) podocytes and (ii) differentiated *APOL1* HR genotype (G1/G2) podocytes versus differentiated *APOL1* LR genotype (G0/G0) podocytes. The numbers of enriched gene ontology molecular function pathways (adjusted *P* value <0.05) from each comparison were 251 and 43 with 28 overlaps (Figure 1e; Supplementary Tables S6 and S7).

The first comparison showed that HUPEC differentiation was associated with higher expression of podocyte marker genes that are included in the list of primary FSGS pathway genes (WikiPathways, WP 2572) than in undifferentiated HUPECs (Figure 1f and g), candidate podocyte marker genes were quantified by RT-qPCR (Supplementary Figure S2). Extracellular matrix related pathway genes were also highly enriched in differentiated podocytes (Figure 1h). This observation suggests an important role for interactions between podocytes and extracellular matrix components and that this interaction could be compromised by podocyte dedifferentiation and loss. This would be consistent with the clinical observation that in progressive glomerular diseases, injured podocytes are lost from the glomerular capillary tuft, into the urinary space.[21]

We next compared expression profiles of the second comparison, differentiated *APOL1* HR genotype (G1/G2) with differentiated *APOL1* LR genotype (G0/G0); we found enriched pathways, including ribosomal and translation-related pathways (Figure 1i). Expression of ribosomal protein coding genes was quantified by RT-qPCR, showing compatible results with RNA-seq, the higher expression levels in differentiated *APOL1* HR genotype (G1/G2) podocytes compared with differentiated *APOL1* LR genotype (G0/G0) podocytes (Supplementary Figure S3). These findings suggest that ribosomal and translation-related pathways may contribute to pathologic mechanisms of *APOL1* HR podocyte upon differentiation *in vitro*.[22]

miRNA Landscape: the Effect of Podocyte Differentiation

Principal component analysis plots of miRNA-seq data showed distinct separation by differentiation status, indicating that differentiation had a robust effect on the miRNA landscape (Figure 2a). The number of differentially expressed miRNAs (selected using an adjusted *P* value <0.05) comparing among differentiation status and by *APOL1* genotypes, was 112 miRNAs and 31 miRNAs, respectively, as shown in Figure 2b–d and Supplementary Tables S8 and S9. We found 17 miRNAs that were differentially expressed by either dedifferentiation or by HR *APOL1* genotype. Of those, 12 miRNAs were downregulated by the combination of dedifferentiation and *APOL1* HR genotype (Figure 2e).

mRNA-miRNA Combined Analysis Showed Potential Interactions

Because each miRNA may reduce expression of multiple mRNA targets, we analyzed both mRNA and miRNA sequencing data together to identify candidate miRNAs specific to differentiation and to *APOL1* genotype. GSEA of total RNA-seq data using the miRNA target prediction database targets module-identified candidate miRNAs that might regulate gene expression for transcripts identified by total RNA-seq. These candidates included 1408 miRNAs, 240 miRNAs, and 170 miRNAs (adjusted *P* value <0.05), when comparing differentiation status in *APOL1* LR, differentiation status in *APOL1* HR, and *APOL1* genotype in differentiated podocytes, respectively (Figure 3a; Supplementary Tables S10–S12).

To validate these candidate miRNAs identified from total RNA-seq data, we matched these candidates with the miRNA-seq data. We identified 15 miRNAs that were downregulated by both differentiation status and by *APOL1* LR genotype (compared with HR), without filtering out miRNA. Of these, 14 miRNAs had less than 100 reads per million mapped reads, except for miR-424-3p (which had 155 reads per million). Of these 15 miRNAs, 10 were among the 1408 miRNAs identified above, which correlated with differentiation of *APOL1* LR podocytes (Figure 3b). In particular, miR-629-3p expression correlated with *APOL1* genotype in differentiated podocytes (and had higher expression in HR podocytes). Furthermore, miR-1285-3p appeared in all 3 GSEA analyses, indicating differential expression and potential regulation of mRNA levels by both differentiation status and *APOL1* genotype (Figure 3c–h). miR-486-5p, miR-629-3p, and miR-1285-3p were quantified by RT-qPCR (Supplementary Figure S4). These candidate miRNAs may be subjects for further studies to determine their functionality in podocytes.

TransferRNA Fragments: Potential Markers for Podocyte Biology

tRNAs represent one of the most abundant classes of cellular RNA transcripts. Processed tRNA fragments represent a recently recognized and growing class of regulatory noncoding RNAs. tRFs exert miRNA-like

functions, including posttranscriptional regulation.[23,24] Taking advantage of miRge3.0 readouts of tRFs, we also conducted differential expression analysis of tRFs to see the effect of differentiation status and *APOL1* genotype.

Principal component analysis plots of tRFs showed separation by HUPEC differentiation status, indicating that cellular differentiation affects tRFs levels (Figure 4a). We defined differentially expressed tRFs as those whose expression levels varied with cell differentiation status or by *APOL1* genotype, with an adjusted *P* value <0.05. This approach identified 106 tRFs whose expression varied by differentiation status and 46 tRFs whose expression varied by *APOL1* genotype (Figure 4b–d; Supplementary Tables S13 and S14).

We categorized differentially expressed tRFs into structural groups according to their origin.[18,24] We noted that tRF-3 was upregulated both with differentiation and with *APOL1*-HR genotype, whereas tRF-1 was downregulated with differentiation (Figure 4e and f). Because tRF-1 derives from cleaved pre-tRNA, tRF-1 downregulation with cell differentiation may indicate reduced proliferation and reduced translational activity in differentiated podocytes, as reported for tRF-1 in prostate cancer cell lines.[25]

Furthermore, we categorized differentially expressed tRFs according to tRNA type. We found that leucine tRFs and methionine (Met) tRFs were downregulated in undifferentiated and *APOL1* HR podocytes (Figure 4g and h). As leucine tRFs regulate translation activity through transcriptional regulation of ribosomal protein mRNA and ribosomal biogenesis,[26,27] and Met tRFs inhibit translation initiation,[28] these differentially expressed tRFs indicate possible translational activity changes in podocytes in response to differentiation status and/or *APOL1* genotype. In contrast, initiator Met tRFs were upregulated in undifferentiated and *APOL1* HR podocytes, suggesting increased proliferation and translational activation. These findings were supported by the comprehensive RNA-seq analysis results presented above, showing translational downregulation in differentiated podocytes and podocytes with *APOL1* LR variant.

Urinary Single-Cell RNA-Seq Data of Podocytes From FSGS Subjects

We previously described the immune signatures of urinary monocytes from FSGS subjects, using single-cell RNA-seq.[19] Here, we investigated the single-cell transcriptomic data of the untransformed podocyte cluster from that study to compare gene expression in cultured transformed HUPECs with HR and LR genotypes

(Figure 5a). We plotted the most differentially expressed genes between *APOL1* HR and LR samples by log-fold change and observed a matching polarity in the expression of these genes in the podocyte cluster (Figure 5b), suggesting that *APOL1* genotype difference is driving this polarity. Using differential gene expression analysis of podocytes, comparing *APOL1* HR and LR podocytes, we identified 158 genes differentially expressed by *APOL1* genotype (Figure 5c). Ingenuity pathway analysis suggested that *APOL1* HR status was associated with activation of elongation initiation factor 2–related and protein kinase R–related pathways (Figure 5d), as we have previously observed in HUPECs.[7]

Furthermore, we performed network building and visualization to connect differentially expressed genes from comparison between differentiated *APOL1* HR HUPECs and differentiated *APOL1* LR HUPECs with differentially expressed genes from urinary single-cell RNA-seq data, comparing *APOL1* HR and LR podocytes. We used both differentially expressed gene sets as input and visualized on STRING human interactome (Figure 6a). We found the ribosomal module and mitochondrial module as distinct modules. *STAT1*, a known upstream regulator of *APOL1* expression, was found to be a highly connected hub gene, possibly mediating the dysregulation of these pathways.[5,29] In addition, we conducted enrichment network analysis to compare differentially expressed genes from RNA-seq from HUPECs with those from single-cell RNA-seq from urinary podocytes. We found that the ribosomal pathway was a common network shared with both data sets (Figure 6b and c).

DISCUSSION

In this study, total RNA-seq, small RNA-seq analyses, and tRF characterizations were applied to 4 HUPECs with known *APOL1* genotype in differentiated and undifferentiated status. We compared the findings with results from urinary single-cell RNA-seq data of podocytes from FSGS subjects. We used the GSEA module to analyze total RNA-seq and small RNA-seq data together. There are several methods available for integrative analysis[30]; we chose GSEA to obtain expression ranking of all genes from total RNA-seq data and matched selected genes with miRNA lists from small RNA-seq data. This approach enabled us to select miRNAs that were likely associated with differentiation status and *APOL1* genotype. Using data from total RNA-seq, we found that *APOL1* HR genotypes (compared with the LR variant) had higher gene expression in ribosomal and translational initiation pathways. Those genes and pathways were also upregulated in undifferentiated podocytes, suggesting that

APOL1 HR genotypes might promote podocyte dedifferentiation.

We also used single-cell RNA-seq data from urinary podocytes obtained from FSGS patients, as recently described.[19] Differential expression analysis showed that the elongation initiation factor 2 pathway was one of the most enriched pathways identified by IPA. This finding suggests enhanced translational activity may contribute to *APOL1* HR genotype-induced podocyte injury. In support of this hypothesis, the elongation initiation factor 2 pathway is one of the pathways dysregulated by APOL1 HR genotype variant proteins.[7,31] We also found that the protein kinase R–related pathway was one of the enriched pathways, supporting previous finding which showed that *APOL1* HR genotype contributes to protein kinase R activation.[7] We observed that the mitochondrial dysfunction pathway was also one of the dysregulated pathways in *APOL1* HR genotype urinary podocytes compared with the LR genotype. Similarly, previous reports showed mitochondrial dysfunction as one of the mechanisms induced by *APOL1* HR genotype.[32-34]

We reported dysregulation of miRNAs in relation to HUPEC differentiation status, *APOL1* genotype, and candidate miRNAs that may be markers of *APOL1* risk-allele–driven dedifferentiation. Podocyte miRNAs have been studied in primary podocytopathy[35] and in the context of *APOL1* variants. Several groups have investigated the role of miR-193a,[36-39] for which we have observed higher expression in differentiated podocytes compared with undifferentiated podocytes. *APOL1* is a predicted target gene for both miR-629-3p and miR-1285-3p, according to the TargetScanHuman 8.0 application.[40] Considering lower *APOL1* expression levels in undifferentiated *APOL1* HR genotype podocyte (Supplementary Figure S5), these 2 miRNAs may be involved in regulating *APOL1* expression levels.

Podocyte tRFs have been recently described in a mouse podocyte cell line.[41,42] The investigators reported that differentiation and doxorubicin exposure induced distinct patterns of differentially expressed tRFs. Here, we characterized differentially expressed tRFs by HUPEC differentiation status and *APOL1* genotype. Our findings suggest that tRF-1 may be a biomarker for differentiation. tRF-1 has been reported to correlate positively with proliferation[25] and to function as a sponge for small RNAs.[43]

Findings from this work concerning downregulation of leucine tRFs and Met tRFs and upregulation of initiator Met tRFs in undifferentiated and *APOL1* HR HUPECs are compatible with prior reports that leucine tRFs regulate translational activity through regulation of ribosomal biogenesis[26,27] and that Met tRFs inhibit translational initiation.[28] Small RNA-seq has been conducted recently on microdissected healthy kidneys and FSGS kidneys, including glomerular samples,[44] but cellular resolution when quantifying small RNA levels in kidney tissue has not been achieved.

The candidate miRNAs and tRFs reported here will require further studies to understand their functions and the potential utility as disease biomarkers. Some molecules may then become biomarkers and/or therapeutic targets for podocyte diseases, including *APOL1* kidney diseases. To understand small RNA function in podocytes, further investigations with techniques allowing cellular resolution are warranted.

This study has limitations. First, it involved an *in vitro* differentiation system using transformed human podocytes that may not recapitulate all aspects of podocyte injury in human diseases. SV40 may not completely be inactivated at 37 °C because the nonpermissive temperature is 39 °C.[45,46] The protein becomes inactive at a lower temperature (37 °C) as our group[1] and another group[47] have shown. This can be the reason for modest level of increased podocyte gene expression and undetectable *NPHS2* RNA expression on differentiation at 37 °C. Second, although we have characterized 4 different podocyte lines with particular *APOL1* genotypes, their origins from individual human subjects are potential confounding factors. We do not have whole-genome sequencing data on these subjects. Third, all cells are from male subjects because we encountered frequent squamous cell contamination in female subjects, which hindered sample analysis. This limits the generalizability of findings in this study and is an important technical problem to be overcome. Fourth, we compared *APOL1* G0/G0 genotype and G1/G2 genotype, but HUPECs with other genotypes such as G1/G1 and G2/G2, were not available. Although we acknowledge these limitations, this study demonstrated consistent transcriptomic changes of human podocyte cell lines by differentiation and by *APOL1* genotype. In conclusion, we have profiled the transcriptomic landscape of human podocytes, including total RNA, miRNA, and tRF, to characterize the effects of differentiation and *APOL1* genotype. Translation-related pathways were identified as pathways likely to be dysregulated by dedifferentiation and *APOL1* HR variants. Further assessment and characterization of the candidate pathways, miRNAs, and tRFs identified here may contribute to better understanding of podocytopathies.

DISCLOSURE

All the authors declared no competing interests.

ACKNOWLEDGMENTS

Data Availability

Original data files and count tables are deposited in GEO (GSE194337). Data are available from the authors upon request.

AUTHOR CONTRIBUTIONS

TY, SS, JH, CAW, and JBK conceived the study design. TY and SS cultured HUPECs. TY analyzed HUPECs data with support by MKH and AZR. KZL and TY analyzed urinary single-cell data. TY, KZL, JBK drafted the manuscript, and all the authors edited the manuscript.

SUPPLEMENTARY MATERIAL

Supplementary File (PDF)
Figure S1. Experimental Methods.
Figure S2. Podocyte marker gene expression levels by RT-qPCR and RNA-seq.
Figure S3. Ribosomal protein coding gene expression levels by RT-qPCR and RNA-seq.
Figure S4. Candidate miRNA levels by RT-qPCR and RNA-seq.
Figure S5. *APOL1* expression levels in podocytes.
Table S1. The sequencing and mapping statistics of total RNA-seq.
Table S2. The sequencing and mapping statistics of small RNA-seq.
Table S3. Primers and probes used for RT-qPCR.
Table S4. Differentially expressed genes (adjusted *P* value <0.05) from comparisons on the basis of the differentiation status.
Table S5. Differentially expressed genes (adjusted *P* value <0.05) from comparisons based on APOL1 genotypes.
Table S6. Enriched gene ontology molecular function (GOMF) pathways (FDR q-value <0.05) from comparison differentiated APOL1 LR genotype (G0/G0) podocytes versus undifferentiated APOL1 LR genotype (G0/G0) podocytes.
Table S7. Enriched gene ontology molecular function (GOMF) pathways (FDR q-value <0.05) from comparison differentiated APOL1 HR genotype (G1/G2) podocytes versus differentiated APOL1 LR genotype (G0/G0) podocytes.
Table S8. Differentially expressed miRNAs (adjusted *P* value <0.05) comparing on the basis of differentiation status.
Table S9. Differentially expressed miRNAs (adjusted *P* value <0.05) comparing based on APOL1 genotypes.
Table S10. Candidate miRNAs by GSEA analysis of total RNA-seq data using the miRNA target prediction database targets module comparing differentiation status in APOL1 LR.
Table S11. Candidate miRNAs by GSEA analysis of total RNA-seq data using the miRNA target prediction database targets module comparing differentiation status in APOL1 HR.
Table S12. Candidate miRNAs by GSEA analysis of total RNA-seq data using the miRNA target prediction database targets module comparing APOL1 genotype in differentiated podocytes.
Table S13. Differentially expressed transfer RNA fragments (adjusted *P* value <0.05) comparing on the basis of differentiation status.
Table S14. Differentially expressed transfer RNA fragments (adjusted *P* value <0.05) comparing based on APOL1 genotype

REFERENCES

1. Sakairi T, Abe Y, Kajiyama H, et al. Conditionally immortalized human podocyte cell lines established from urine. *Am J Physiol Ren Physiol*. 2010;298:F557–F567. https://doi.org/10.1152/ajprenal.00509.2009

2. Okamura K, Dummer P, Kopp J, et al. Endocytosis of albumin by podocytes elicits an inflammatory response and induces apoptotic cell death. *PLoS One*. 2013;8:e54817. https://doi.org/10.1371/journal.pone.0054817

3. Dobrinskikh E, Okamura K, Kopp JB, Doctor RB, Blaine J. Human podocytes perform polarized, caveolae-dependent albumin endocytosis. *Am J Physiol Ren Physiol*. 2014;306:F941–F951. https://doi.org/10.1152/ajprenal.00532.2013

4. Kumar S, Tikoo K. Independent role of PP2A and mTORc1 in palmitate induced podocyte death. *Biochimie*. 2015;112:73–84. https://doi.org/10.1016/j.biochi.2015.02.009

5. Beckerman P, Bi-Karchin J, Park AS, et al. Transgenic expression of human APOL1 risk variants in podocytes induces kidney disease in mice. *Nat Med*. 2017;23:429–438. https://doi.org/10.1038/nm.4287

6. Wu J, Raman A, Coffey NJ, et al. The key role of NLRP3 and STING in APOL1-associated podocytopathy. *J Clin Invest*. 2021;131:e136329. https://doi.org/10.1172/JCI136329

7. Okamoto K, Rausch JW, Wakashin H, et al. APOL1 risk allele RNA contributes to renal toxicity by activating protein kinase R. *Commun Biol*. 2018;1:188. https://doi.org/10.1038/s42003-018-0188-2

8. Ge M, Molina J, Ducasa GM, et al. APOL1 risk variants affect podocyte lipid homeostasis and energy production in focal segmental glomerulosclerosis. *Hum Mol Genet*. 2021;30:182–197. https://doi.org/10.1093/hmg/ddab022

9. Uzureau S, Lecordier L, Uzureau P, et al. APOL1 C-terminal variants may trigger kidney disease through interference with APOL3 control of actomyosin. *Cell Rep*. 2020;30:3821–3836. e13. https://doi.org/10.1016/j.celrep.2020.02.064

10. Freedman BI, Kopp JB, Sampson MG, Susztak K. APOL1 at 10 years: progress and next steps. *Kidney Int*. 2021;99:1296–1302. https://doi.org/10.1016/j.kint.2021.03.013

11. Martin M. Cutadapt removes adapter sequences from high-throughput sequencing reads. *EMBnet J*. 2011;17. https://doi.org/10.14806/ej.17.1.200

12. Dobin A, Davis CA, Schlesinger F, et al. STAR: ultrafast universal RNA-seq aligner. *Bioinformatics*. 2013;29:15–21. https://doi.org/10.1093/bioinformatics/bts635

13. Li B, Dewey CN. RSEM: accurate transcript quantification from RNA-Seq data with or without a reference genome. *BMC Bioinformatics*. 2011;12:323. https://doi.org/10.1186/1471-2105-12-323

14. Subramanian A, Tamayo P, Mootha VK, et al. Gene set enrichment analysis: a knowledge-based approach for interpreting genome-wide expression profiles. *Proc Natl Acad Sci U S A*. 2005;102:15545–15550. https://doi.org/10.1073/pnas.0506580102

15. Mootha VK, Lindgren CM, Eriksson KF, et al. PGC-1alpha-responsive genes involved in oxidative phosphorylation are coordinately downregulated in human diabetes. *Nat Genet*. 2003;34:267–273. https://doi.org/10.1038/ng1180

16. Stein CB, Genzor P, Mitra S, et al. Decoding the 5′ nucleotide bias of PIWI-interacting RNAs. *Nat Commun*. 2019;10:828. https://doi.org/10.1038/s41467-019-08803-z

17. Patil AH, Halushka MK. miRge3.0: a comprehensive micro-RNA and tRF sequencing analysis pipeline. *NAR Genom Bioinform*. 2021;3:lqab068. https://doi.org/10.1093/nargab/lqab068

18. Looney MM, Lu Y, Karakousis PC, Halushka MK. *Mycobacterium tuberculosis* infection drives mitochondria-biased dysregulation of host transfer RNA-derived fragments. *J Infect Dis*. 2021;223:1796–1805. https://doi.org/10.1093/infdis/jiaa596

19. Latt KZ, Heymann J, Jessee JH, et al. Urine single-cell RNA sequencing in focal segmental glomerulosclerosis reveals inflammatory signatures. *Kidney Int Rep*. 2021;7:289–304. https://doi.org/10.1016/j.ekir.2021.11.005

20. Zhou G, Soufan O, Ewald J, et al. NetworkAnalyst 3.0: a visual analytics platform for comprehensive gene expression profiling and meta-analysis. *Nucleic Acids Res*. 2019;47:W234–W241. https://doi.org/10.1093/nar/gkz240

21. Yin L, Yu L, He JC, Chen A. Controversies in podocyte loss: death or detachment? *Front Cell Dev Biol*. 2021;9:771931. https://doi.org/10.3389/fcell.2021.771931

22. May CJ, Saleem M, Welsh GI. Podocyte dedifferentiation: a specialized process for a specialized cell. *Front Endocrinol (Lausanne)*. 2014;5:148. https://doi.org/10.3389/fendo.2014.00148

23. Kuscu C, Kumar P, Kiran M, Su Z, Malik A, Dutta A. tRNA fragments (tRFs) guide Ago to regulate gene expression post-transcriptionally in a Dicer-independent manner. *RNA*. 2018;24:1093–1105. https://doi.org/10.1261/rna.066126.118

24. Magee R, Rigoutsos I. On the expanding roles of tRNA fragments in modulating cell behavior. *Nucleic Acids Res*. 2020;48:9433–9448. https://doi.org/10.1093/nar/gkaa657

25. Lee YS, Shibata Y, Malhotra A, Dutta A. A novel class of small RNAs: tRNA-derived RNA fragments (tRFs). *Genes Dev*. 2009;23:2639–2649. https://doi.org/10.1101/gad.1837609

26. Kim HK, Fuchs G, Wang S, et al. A transfer-RNA-derived small RNA regulates ribosome biogenesis. *Nature*. 2017;552:57–62. https://doi.org/10.1038/nature25005

27. Kim HK, Xu J, Chu K, et al. A tRNA-derived small RNA regulates ribosomal protein S28 protein levels after translation initiation in humans and mice. *Cell Rep*. 2019;29:3816–3824. e4. https://doi.org/10.1016/j.celrep.2019.11.062

28. Ivanov P, Emara MM, Villen J, et al. Angiogenin-induced tRNA fragments inhibit translation initiation. *Mol Cell*. 2011;43:613–623. https://doi.org/10.1016/j.molcel.2011.06.022

29. Davis SE, Khatua AK, Popik W. Nucleosomal dsDNA stimulates APOL1 expression in human cultured podocytes by activating the cGAS/IFI16-STING signaling pathway. *Sci Rep*. 2019;9:15485. https://doi.org/10.1038/s41598-019-51998-w

30. Nazarov PV, Kreis S. Integrative approaches for analysis of mRNA and microRNA high-throughput data. *Comput Struct Biotechnol J*. 2021;19:1154–1162. https://doi.org/10.1016/j.csbj.2021.01.029

31. Datta S, Kataria R, Zhang JY, et al. Kidney disease-associated APOL1 variants have dose-dependent, dominant toxic gain-of-function. *J Am Soc Nephrol*. 2020;31:2083–2096. https://doi.org/10.1681/ASN.2020010079

32. Ma L, Chou JW, Snipes JA, et al. APOL1 renal-risk variants induce mitochondrial dysfunction. *J Am Soc Nephrol*. 2017;28:1093–1105. https://doi.org/10.1681/ASN.2016050567

33. Granado D, Muller D, Krausel V, et al. Intracellular APOL1 risk variants cause cytotoxicity accompanied by energy depletion. *J Am Soc Nephrol*. 2017;28:3227–3238. https://doi.org/10.1681/ASN.2016111220

34. Shah SS, Lannon H, Dias L, et al. APOL1 kidney risk variants induce cell death via mitochondrial translocation and opening of the mitochondrial permeability transition pore. *J Am Soc Nephrol*. 2019;30:2355–2368. https://doi.org/10.1681/ASN.2019020114

35. Iranzad R, Motavalli R, Ghassabi A, et al. Roles of microRNAs in renal disorders related to primary podocyte dysfunction.

Life Sci. 2021;277:119463. https://doi.org/10.1016/j.lfs.2021.119463

36. Ekulu PM, Adebayo OC, Decuypere JP, et al. Novel human podocyte cell model carrying G2/G2 APOL1 high-risk genotype. *Cells*. 2021;10:1914. https://doi.org/10.3390/cells10081914

37. Jha A, Saha S, Ayasolla K, et al. MiR193a modulation and podocyte phenotype. *Cells*. 2020;9:1004. https://doi.org/10.3390/cells9041004

38. Mishra A, Ayasolla K, Kumar V, et al. Modulation of apolipoprotein L1-microRNA-193a axis prevents podocyte dedifferentiation in high-glucose milieu. *Am J Physiol Ren Physiol*. 2018;314:F832–F843. https://doi.org/10.1152/ajprenal.00541.2017

39. Kumar V, Ayasolla K, Jha A, et al. Disrupted apolipoprotein L1-miR193a axis dedifferentiates podocytes through autophagy blockade in an APOL1 risk milieu. *Am J Physiol Cell Physiol*. 2019;317:C209–C225. https://doi.org/10.1152/ajpcell.00538.2018

40. McGeary SE, Lin KS, Shi CY, et al. The biochemical basis of microRNA targeting efficacy. *Science*. 2019;366:eaav1741. https://doi.org/10.1126/science.aav1741

41. Shi H, Yu M, Wu Y, et al. tRNA-derived fragments (tRFs) contribute to podocyte differentiation. *Biochem Biophys Res Commun*. 2020;521:1–8. https://doi.org/10.1016/j.bbrc.2019.09.009

42. Li S, Liu Y, He X, et al. tRNA-derived fragments in podocytes with adriamycin-induced injury reveal the potential mechanism of idiopathic nephrotic syndrome. *Biomed Res Int*. 2020;2020:7826763. https://doi.org/10.1155/2020/7826763

43. Lalaouna D, Carrier MC, Semsey S, et al. A 3′ external transcribed spacer in a tRNA transcript acts as a sponge for small RNAs to prevent transcriptional noise. *Mol Cell*. 2015;58:393–405. https://doi.org/10.1016/j.molcel.2015.03.013

44. Williams AM, Jensen DM, Pan X, et al. Histologically resolved small RNA maps in primary focal segmental glomerulosclerosis indicate progressive changes within glomerular and tubulointerstitial regions. *Kidney Int*. 2022;101:766–778. https://doi.org/10.1016/j.kint.2021.12.030

45. Hardy K, Mansfield L, Mackay A, et al. Transcriptional networks and cellular senescence in human mammary fibroblasts. *Mol Biol Cell*. 2005;16:943–953. https://doi.org/10.1091/mbc.e04-05-0392

46. O'Hare MJ, Bond J, Clarke C, et al. Conditional immortalization of freshly isolated human mammary fibroblasts and endothelial cells. *Proc Natl Acad Sci U S A*. 2001;98:646–651. https://doi.org/10.1073/pnas.98.2.646

47. Saleem MA, O'Hare MJ, Reiser J, et al. A conditionally immortalized human podocyte cell line demonstrating nephrin and podocin expression. *J Am Soc Nephrol*. 2002;13:630–638. https://doi.org/10.1681/asn.V133630